nature COMMUNICATIONS

ARTICLE

Received 22 Mar 2013 | Accepted 28 Oct 2013 | Published 22 Nov 2013

DOI: 10.1038/ncomms3829

miR-1 and miR-206 target different genes to have opposing roles during angiogenesis in zebrafish embryos

Cheng-Yung Lin[1,*], Hung-Chieh Lee[1,*], Chuan-Yang Fu[1,*], Yu-Yun Ding[1], Jie-Shin Chen[1], Ming-Hsuan Lee[1], Wei-Jhen Huang[1] & Huai-Jen Tsai[1,2]

As *miR-1* and *miR-206* share identical seed sequences, they are commonly speculated to target the same gene. Here, we identify an mRNA encoding seryl-tRNA synthetase (SARS), which is targeted by *miR-1,* but refractory to *miR-206*. SARS is increased in *miR-1*-knockdown embryos, but it remains unchanged in the *miR-206* knockdown. Either *miR-1* knockdown or *sars* overexpression results in a failure to develop some blood vessels and a decrease in vascular endothelial growth factor Aa (VegfAa) expression. In contrast, *sars* knockdown leads to an increase of VegfAa expression and abnormal branching of vessels, similar to the phenotypes of *vegfaa*-overexpressed embryos, suggesting that *miR-1* induces angiogenesis by repressing SARS. Unlike the few endothelial cells observed in the *miR-1*-knockdown embryos, knockdown of *miR-206* leads to abnormal branching of vessels accompanied by an increase in endothelial cells and VegfAa. Therefore, we propose that *miR-1* and *miR-206* target different genes and thus have opposing roles during embryonic angiogenesis in zebrafish.

[1] Institute of Molecular and Cellular Biology, National Taiwan University, Taipei 10617, Taiwan. [2] Research Center for Developmental Biology and Regenerative Medicine, National Taiwan University, Taipei 10617, Taiwan. * These authors contributed equally to this work. Correspondence and requests for materials should be addressed to H.-J.T. (email: hjtsai@ntu.edu.tw).

MicroRNAs (*miRNAs*) are single-stranded RNA molecules, about 19–30 nucleotides (nt) in length, which repress the expression of their target genes through binding mRNAs at specific sequences. They control gene expression at post-translational level by various mechanisms, such as decay of mRNAs and blockage of translation[1–3]. Bioinformatics studies indicate that expressions of 30∼50% of human genes are probably controlled by *miRNAs*[4,5]. Therefore, to understand the exact relationship between genes and their functions in embryos, it is necessary to clearly identify the target genes of specific *miRNAs* at particular developmental stages.

miR-1 (*miR-1-1* and *miR-1-2*) and *miR-206* are known as highly conserved *miRNAs* which share common expression in the muscles of organisms ranging from *Caenorhabditis elegans* to human[6]. However, *miR-1-1, miR-1-2* and *miR-206* are located at three different chromosomal regions, including 20q13.33, 18q11.2 and 6p12.2, respectively, in the human genome[7]. More specifically, although *miR-1-1* locates at the intron of the *C20orf166* gene, *miR-1-2* locates at the intron of the *Mindbomb* gene, and *miR-206* locates in the intergenic region[8,9]. Moreover, *miR-1* and *miR-206* have different pre-*miRNA* sequences, and they differ by four nt at mature *miRNA*[7]. It is also reported that *miR-1* and *miR-206* have different regulatory pathways. For example, overexpression of Myf5 and Myogenin in the neural tube can induce ectopic expressions of *miR-1* and *miR-206*, whereas overexpression of Myod can induce only *miR-1* (ref. 6). *miR-1* and *miR-206* have different regulatory functions within the dystrophin/nNOS pathway[10]. These facts suggest that *miR-1* and *miR-206* may have different roles in gene regulation. Yet, as *miR-1* and *miR-206* share identical seed sequence, the results of any given bioinformatics search would predict the same target genes. Consequently, *miR-1* and *miR-206* are commonly speculated to have identical biological functions and are therefore considered to act conjointly as a single regulator termed as *miR-1/206*. For example, *miR-1/206* regulates *connexin43* expression during skeletal muscle development[11]. *miR-1/206* can repress vascular endothelial growth factor Aa gene (*vegfaa*) expression[12]. Therefore, whether *miR-1* and *miR-206* act separately to regulate different genes or act together to regulate the same genes remains controversial.

In vitro studies suggested that *miR-1* and *miR-206* promote myoblast differentiation[7]. In zebrafish, *miR-1* and *miR-206* function in muscle gene expression and regulate sarcomeric actin organization[13]. Moreover, many factors, such as Seryl-transfer RNA synthetase (SARS)[14] and fibroblast growth factor signalling[15,16], mediate Vegf expression in somites during embryogenesis. Nakasa *et al.*[17] reported that *miR-1, -133* and *-206* in muscle enhance angiogenesis during muscle regeneration. In contrast, Stahlhut *et al.*[12] found that *miR-1/206* in muscle negatively regulates developmental angiogenesis through the repression of VegfAa expression. As no consensus has thus far been reached with respect to the regulatory function(s) of *miR-1/206*, we conducted a more intensive examination of the molecular mechanism underlying the activity of these muscle-specific *miRNAs* in modulating angiogenesis during zebrafish embryonic development. To accomplish this, we employed the labelled miRNA pull-down (LAMP) assay system[18] to obtain the target genes specific for *miR-1* and *miR-206*.

Here, we found the endogenous *sars*-3′-untranslated region (*sars*-3′UTR) target sequence (outside of seed) is refractory to *miR-206* targeting, despite additional *miR-206* complementarity. Instead, *sars*-3′UTR target sequence is specifically targeted by *miR-1*. Additionally, the *vegfaa*-3′UTR is only targeted by *miR-206* but not *miR-1*. Therefore, *miR-1* and *miR-206* act as independent upstream regulators, increasing or decreasing *vegfaa* expression, respectively, to ultimately have opposing roles in zebrafish angiogenesis. Our work points to specificity constraints that depend on the target sequence outside of the seed of *miR-1* and *miR-206*.

Results

Identification of putative target genes of mature *miR-1*. Using the LAMP assay system and microarray analysis, we have previously searched all the putative target genes of mature *miR-1* (ref. 18). Here, we went further to focus on the candidate genes which are expressed in the muscle during zebrafish embryogenesis. The 3′UTR of these candidate genes for all 7-mer and 8-mer sequences complementary to zebrafish *miR-1* seeds were searched by using RNAhybrid software[19]. Among 302 putative target genes for *miR-1*, 88 are categorized as muscle-specific genes. We selected eight of them to perform luciferase (*luc*) assays. These 3′UTR cDNAs were individually cloned and engineered to fuse at the downstream of *luc* reporter gene and transfected together with *miR-1* into cell lines C2C12 and HEK293T. Among them, the S-adenosylhomocysteine hydrolase gene was equally regulated by *miR-1* and *miR-206*, whereas eukaryotic translation initiation factor 2 subunit 1 alpha gene was neither regulated by *miR-1* nor *miR-206* (Supplementary Fig. S1). Interestingly, as the *luc* activity was repressed in the construct containing 3′UTR of succinate-CoA ligase gene (*suclg1*) and *sars*, they were determined to be targets of *miR-1* with high potential (Supplementary Fig. S1). Unexpectedly, we found that *sars* and *suclg1* were regulated by *miR-1* and that the spatiotemporal expressions of *suclg1 and sars-mRNA* were all detected in the somites of embryos at 20, 24 and 48 hours post-fertilization (hpf; Supplementary Fig. S1). As the *luc* assay demonstrated that *sars* was repressed effectively by *miR-1*, we chose *sars* to perform the following experiments in more detail.

The *sars*-mRNA is bound and regulated by *miR-1* only. The 3′UTRs of zebrafish, mouse and human *sars* were individually

Figure 1 | Only *miR-1* specifically inhibits *sars* expression *in vitro* and *in vivo*. (**a**) Diagrams of the *luc* reporter constructs containing *sars*-3′UTRs from different species such as zebrafish (Z); mouse (M) and human (H). (**b**) Histograms presented the *luc* activity obtained from HEK-293T and C2C12 cells when *miR-1* was co-transfected with plasmids as indicated. The phRL-*myf5* vector served as a control group, and its *luc* activity was set to 1. (**c**) Histograms presented the *luc* activity obtained from C2C12 cells when *miR-206* was co-transfected with plasmids as indicated. The phRL-*myf5* vector served as a control group, and its *luc* activity was set to 1. (**d**) Diagrams of the *luc* reporter constructs containing Wt and mutated *sars*-3′UTRs. The mutated sequence was labelled with red. The seed sequence was blocked with green. (**e**) Histograms presented the *luc* activity obtained from embryos at 24 hpf. Plasmid phRL-*myf5* vector served as a control group, and its *luc* activity was set to 1. The *luc* activity assay in panels (**b**), (**c**) and (**e**) are calculated from three independent experiments and presented as mean ± s.d. ($n=3$). Student's *t*-test was used to determine significant differences between each construct and control within each group (***$P<0.005$). (**f**) The sequences of pre-*miR-1* and pre-*miR-206* were aligned to *miR-1*-MO1 and *miR-206*-MO, respectively, as shown. WISH of *miR-1* and *miR-206* in WT, *miR-1*-MO1- and *miR-206*-MO-injected embryos was examined at 30 hpf. Scale bar presents 300 μm. (**g**) The patterns of SARS protein in WT and embryos injected with control-MO (8 ng), *miR-1*-MO1 (8 ng), *miR-1*-MO2 (8 ng), *miR-206*-MO (8 ng) and *miR-1/206*-MO (8 ng) at 48 hpf by western blot analysis. GAPDH was used as an internal control. (**h**) Statistical analysis of the average relative intensity of SARS protein from each group was presented. Data are calculated from three independent experiments and presented as mean ± s.d. ($n=3$). Student's *t*-test was used to determine significant differences between each construct and control within each group (***$P<0.005$ and **$P<0.01$).

cloned and fused at the downstream of *luc* reporter gene (Fig. 1a). After these constructs were transfected separately, together with *miR-1*, into human HEK293T cells, the *luc* activity was significantly decreased by 42% and 35% in the constructs containing zebrafish and human *sars*-3′UTRs, respectively (Fig. 1b). Similarly, in mouse C2C12 cells, the *luc* activity was significantly decreased by 47% and 36% in the construct containing zebrafish and mouse *sars*-3′UTRs, respectively (Fig. 1b), suggesting that *miR-1* can bind to *sars*-3′UTR, resulting in the reduction of reporter activity. However, the *luc* activities fused with *sars*-3′UTRs from zebrafish and mouse remained unchanged when each construct was cotransfected with *miR-206* into C2C12 cells (Fig. 1c), suggesting that *sars*-3′UTR is specifically bound by *miR-1*, but not by *miR-206*.

We further studied whether *sars*-3′UTR is only regulated by endogenous *miR-1* in zebrafish embryos. To accomplish this, we constructed plasmid phRL-*myf5*-Z*sars*-3′UTR, in which a zebrafish *sars*-3′UTR was fused with *luc* reporter and driven by zebrafish *myf5* promoter to serve as a control group (Fig. 1d,e). A mutated plasmid, phRL-*myf5*-Z*sars*-3′UTR-mt1, was also constructed, in which the predicted target sites for *miR-1*, that is, TTCA located at +2,024 to +2,027 nt, were mutated into

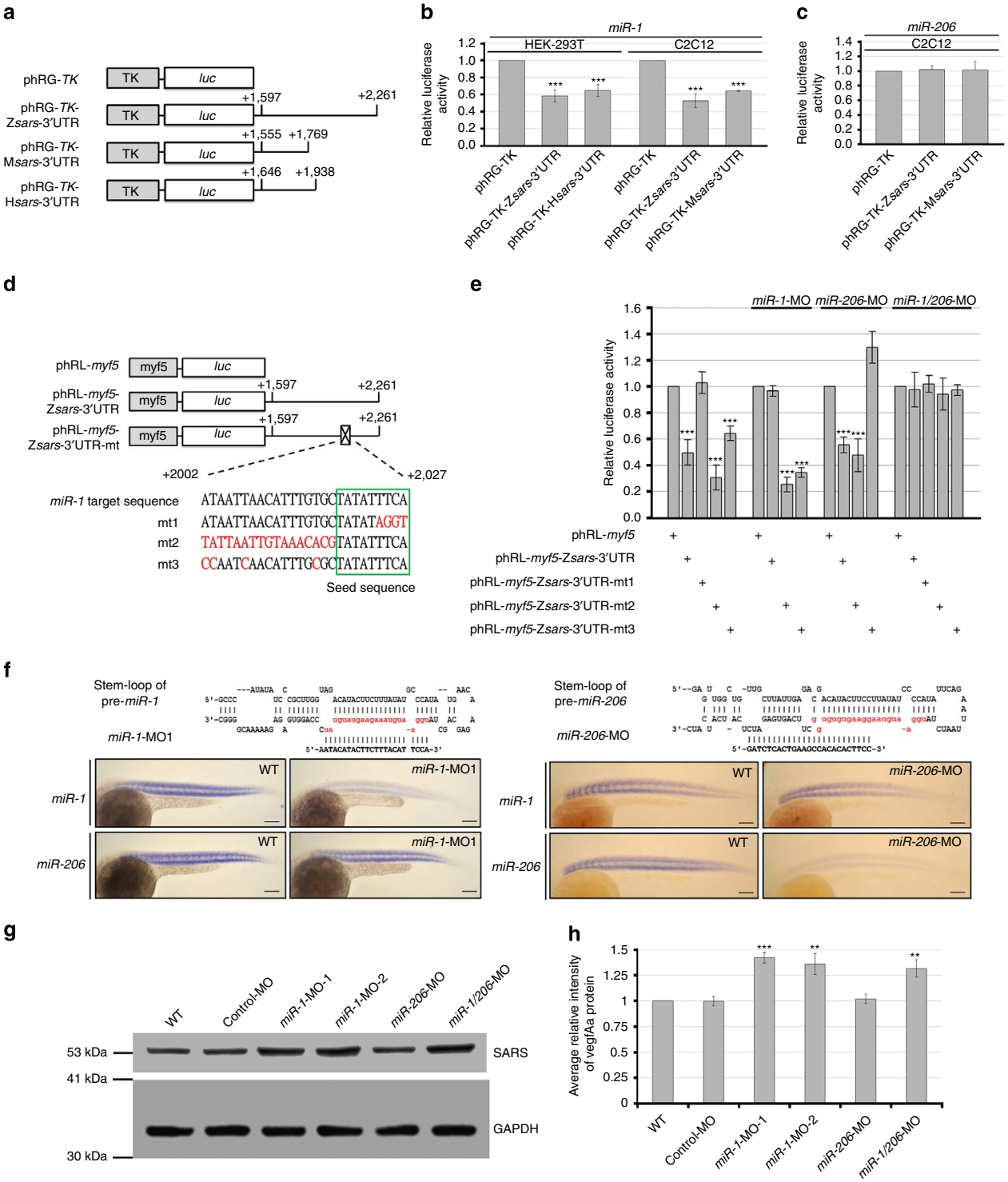

AGGT (Fig. 1d). Compared with the control group, the *luc* activity of the embryos injected with phRL-*myf5*-Z*sars*-3′UTR was greatly decreased by 55%, whereas that of embryos injected with phRL-*myf5*-Z*sars*-3′UTR-mt1 remained unchanged (Fig. 1e), indicating that mutation of *miR-1* target sequences resulted in abolishing the repression of *miR-1*, allowing it to bind and silence *sars,* both *in vitro* and *in vivo*.

In addition, we designed *miR-1*-MO1, *miR-1*-MO2, *miR-206*-MO and *miR-1/206*-MO, which simultaneously knockdown both *miR-1* and *miR-206*, as well as control-MO, for further experiments (Supplementary Fig. S3). Whole-mount *in situ* hybridization (WISH) showed that the *miR-1* was only absent in the *miR-1*-MO1- and *miR-1*-MO2-injected embryos, whereas *miR-206* was only absent in the *miR-206*-MO-injected embryos (Fig. 1f and Supplementary Fig. S3), indicating that the MOs we used were specific for *miR-1* and *miR-206* individually. When *miR-1* was knocked down by injection of *miR-1*-MO1, the *luc* activity of embryos injected with phRL-*myf5*-Z*sars*-3′UTR was close to that of control phRL-*myf5*-injected embryos (Fig. 1e), suggesting that the endogenous *miR-1* was reduced by introducing *miR-1*-MO1 and lost its ability to silence phRL-*myf5*-Z*sars*-3′UTR in embryos. When embryos were injected with phRL-*myf5*-Z*sars*-3′UTR plus *miR-206*-MO, *luc* activity continued to decrease (Fig. 1e), indicating that *miR-206* was not involved in silencing the injected phRL-*myf5*-Z*sars*-3′UTR in embryos. These findings further suggest that *sars*-3′UTR is regulated by endogenous *miR-1*, not *miR-206*, in zebrafish embryos.

On the basis of the prediction of bioinformatics software, such as RNAhybrid[19], the complementarity between the target sequence (+2,002 to +2,027) and each *miRNA* is shown in Supplementary Fig. S4. To demonstrate that both seed and sequences in the neighbourhood of the seed are involved in the specificity of *miRNA* differential targeting, we constructed two plasmids: phRL-*myf5*-Zsars-3′UTR-mt2 and phRL-*myf5*-Zsars-3′UTR-mt3. The first plasmid contains a mutated sequence in the 3′UTR of *sars* whose *miR-1* target sequence outside the seed is altered, whereas the second plasmid contains a mutated sequence in the 3′UTR of *sars* whose *miR-1* target site is altered such that a base pair extensively matches that of *miR-206*. Compared with control, the *luc* activity was also greatly reduced in embryos injected with phRL-*myf5*-Zsars-3′UTR-mt2 (Fig.1e). However, this reduction could not be restored by knocking down either *miR-1* or *miR-206* (Fig. 1e), indicating that the mutated sequence outside the seed sequence of *miR-1* leads to failure in selecting a specific target for *miR-1*. Furthermore, the *luc* activity of dual *miR-1*/*miR-206* knockdown embryos was close to that of embryos injected with phRL-*myf5* (control), embryos injected with phRL-*myf5*-Z*sars*-3′UTR and embryos injected with mt2 mutated constructs (Fig. 1e). Thus, both *miR-1* and *miR-206* target the same site, in turn reducing *luc* activity (Fig. 1e). These data indicates that a target outside the seed sequence of *miR-1* is a critical factor related to the selection of either *miR-1* or *miR-206* targeting. Importantly, when we injected embryos with phRL-*myf5*-Zsars-3′UTR-mt3 altered in the manner suggested above, the *luc* activity was still reduced in *miR-1*-knockdown embryos, but fully restored in *miR-206*- and *miR-1/206*-knockdown embryos, compared with control group (Fig. 1e). These data indicate that a difference of only four nt between *miR-1* and *miR-206* becomes a sequence that is determinative of the differential targeting between *miR-1* and *miR-206*.

We also analysed the protein levels of SARS in embryos injected with control-MO, *miR-1*-MO1, *miR-1*-MO2, *miR-206*-MO and *miR-1/206*-MO. Results showed that the SARS protein level was increased in embryos injected *miR-1*-MO1 (average relative intensity (ari) ± standard deviation (s.d.) was 1.42 ± 0.05), *miR-1*-MO2 (ari ± s.d. = 1.36 ± 0.10) and *miR-1/206*-MO (ari ± s.d. = 1.32 ± 0.09) relative to that of embryos injected with control-MO (ari ± s.d. = 0.99 ± 0.05). Similar to the *luc* data, embryos injected with *miR-206*-MO did not show any change in SARS protein level (ari ± s.d. = 1.02 ± 0.05) (Fig. 1g,h). Together, we concluded that *miR-1,* but not *miR-206,* regulates *sars* expression during zebrafish development.

***miR-1* promotes angiogenesis through reducing SARS protein.** In zebrafish, the non-canonical activity of SARS in somites is involved in the vascular development through modulating the expression of *vegfaa*[14,20]. Our data showed that knockdown of *miR-1* can increase SARS protein level in embryos, suggesting that excessive SARS may, in turn, repress *vegfaa* expression to affect angiogenesis. To prove this hypothesis, we performed either knockdown of *miR-1* or overexpression of *sars*-mRNA and analysed vascular development using the transgenic line *Tg(fli-EGFP)*^{y1} whose endothelial cells are labelled by enhanced green fluorescent protein (EGFP). In the uninjected control embryos during 30–72 hpf, we observed that (1) the blood vessels crossed the transverse myoseptum to form parachordal vessels (PAVs) and (2) most intersegmental vessels (ISVs) grew rostrally from dorsal aorta and then extended caudally, following the chevron-like contours of the somites to reach the dorsal–lateral surface where tubes from adjacent ISVs fused to form dorsal longitudinal anastomotic vessels (Fig. 2a). However, in the *miR-1* morphants (Fig. 2b), *sars*-mRNA-injected embryos (Fig. 2c), and *T429A*-mRNA-injected embryos, a *sars* mutated form absent in serine binding (Fig. 2d)[14], we found that (1) the development of ISVs was terminated and stacked at the myoseptal midpoint during 30 hpf, (2) ISVs were misdirected and appeared laterally asymmetrical, (3) PAVs grew slowly, and, finally, (4) PAV and DLAV were incompletely formed during 48 and 72 hpf. These data indicate that either the overexpression of SARS or the induction of SARS expression by introducing *miR-1*-MO1 causes the absence of developing blood vessels in embryos. In addition, the *miR-1*-MO1 phenotype could be rescued by coinjecting an excessive amount of *sars*-MO (Fig. 2b versus f). Unlike the *miR-1*-morphants, which were unable to continue development of blood vessels, the trunk vasculatures were almost completely formed in *miR-1*/*sars*-MO-injected embryos. Ectopic sprouting of the tip cells was detected (white arrowheads of Fig. 2f), which was similar to the phenotypes of *sars* morphants. On the other hand, either knockdown of *sars* by injection of *sars*-MO (Fig. 2e) or overexpression of VegfAa by injection of *vegfaa*-mRNA (Fig. 2i) led to abnormally branched blood vessels among ISVs in trunk during 30–72 hpf (Fig. 2e,h). Furthermore, the phenotype was specific to *miR-1* downregulation, as evidenced by the following observations. First, the defects could be phenocopied by coinjection of *miR-1*-MO1 and *p53*-MO. Second, the defects were not seen in either standard control MO-injected embryos or *miR-1*-5mis-MO-injected embryos (Supplementary Fig. S5). Our data demonstrated that *miR-1* induces angiogenesis through repressing SARS expression during embryonic development.

***miR-206* inhibits angiogenesis during zebrafish embryogenesis.** Although Stahlhut *et al.*[12] reported that *miR-1/206* in muscle negatively regulates developmental angiogenesis, it is unclear whether *miR-206* has an independent role in angiogenesis. To address this question, we employed MOs which can specifically knockdown *miR-1* or/and *miR-206* (Fig. 1f). Embryos injected with *miR-206*-MO (Fig. 2g) or *miR-1/206*-MO (Fig. 2h) led to abnormally branched blood vessels among ISVs in trunk during 30–72 hpf. In addition, similar to the uninjected control embryos (Fig. 2j), three to four endothelial cells were observed in the *Tg(fli-nuclearGFP)*^{y7} embryos injected with *miR-1*-MO1 during

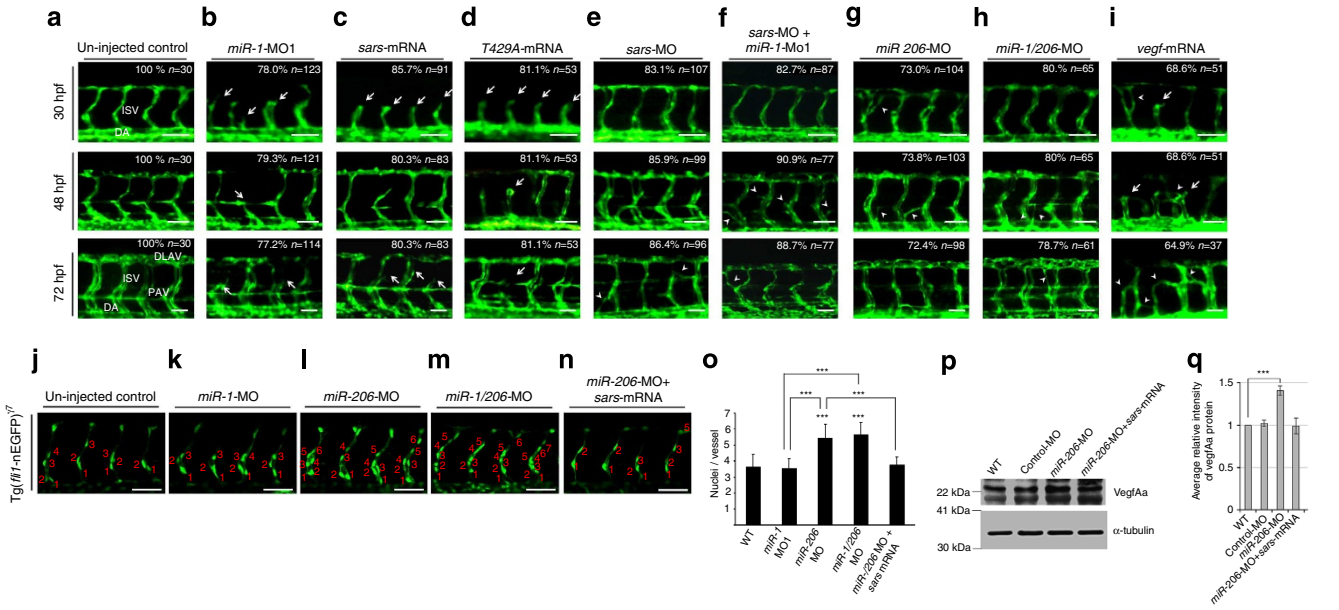

Figure 2 | Distinct functions of *miR-1* and *miR-206* in angiogenesis during zebrafish embryonic development. (**a**) Embryos derived from transgenic line *Tg* (*fli1:EGFP*) without treatment served as control. These embryos were injected with (**b**) 8 ng of *miR-1*-MO1, (**c**) 300 pg of *sars*-mRNA, (**d**) 300 pg of *T429A*-mRNA, (**e**) 4 ng of *sars*-MO, (**f**) 6 ng of *miR-1*-MO1 plus 3 ng of *sars*-MO, (**g**) 8 ng of *miR-206*-MO, (**h**) 8 ng of *miR-1/206*-MO and (**i**) 50 pg of *vegf*121-mRNA. All the embryos were observed at 30, 48 and 72 hpf. (**j**–**n**) Embryos derived from line *Tg(fli-nGFP)*^{y7} without treatment served as control. Each nucleus was marked with a number. The total number of nuclei was counted in (**j**) uninjected control embryos and in embryos injected with (**k**) *miR-1*-MO1, (**l**) *miR-206*-MO, (**m**) *miR-1/206*-MO or (**n**) *miR-206*-MO/*sars*-mRNA. (**o**) Statistical analyses of the average number of nuclei per ISV among *miR-1*-MO1-, *miR-206*-MO-, *miR-1/206*-MO- and *miR-206*-MO/*sars*-mRNA-injected embryos at 30 hpf were indicated. Data are calculated from three independent experiments and presented as mean ± s.d. ($n = 3$). (**p**) The patterns of SARS protein in WT and embryos injected with control-MO, *miR-206*-MO and *miR-206*-MO/*sars*-mRNA at 48 hpf, by western blot analysis. α-tubulin was used as an internal control. (**q**) Statistical analysis of the average relative intensity (ari) of SARS protein level from each group was presented. Data are calculated from three independent experiments and presented as mean ± s.d. ($n = 3$). Student's *t*-test was used to determine significant differences between each group (***$P < 0.005$). ISV, intersegmental vessel; DLAV, dorsal longitudinal anastomotic vessel; PAV, parachordal vessel; DA, dorsal aorta; scale bar, 100 μm.

24–28 hpf (Fig. 2k). However, either single knockdown of *miR-206* (Fig. 2l, Supplementary Fig. S6) or double knockdown of *miR-1/206* (Fig. 2m) led to the abnormal branching in trunk blood vessels accompanied by a significant increase in the number of endothelial cells to as many as seven at the same stage (Fig. 2m,o). The result for *miR-1/206*-MO-injected embryos was consistent with Stahlhut *et al.*[12] who reported that the number of endothelial cells in *miR-1/206*-MO-injected embryos was increased. Live imaging analyses of control-MO, *miR-1*-MO1- and *miR-206*-MO-injected embryos derived from line *Tg(fli-nuclearGFP)*^{y7} revealed that the increase of cell number in the *miR-206*-knockdown embryos resulted from enhanced endothelial cell migration as well as elevated cell proliferation, once endothelial cells entered the intersomitic region. In contrast, knockdown of *miR-1* had no effect on endothelial cell behaviour. Instead, angiogenesis was repressed in embryos without *miR-1*. In addition, overexpression of *sars*-mRNA could rescue the pro-angiogenic effects caused by injection of *miR-206*-MO (Fig. 2n,o), indicating that changes in SARS protein level can influence *miR-206*-mediated anti-angiogenic effects. Furthermore, we demonstrated that the protein level of VegfAa was increased (ari ± s.d. = 1.41 ± 0.06) in the embryos injected with *miR-206*-MO, compared with that of control-MO-injected embryos (ari ± s.d. = 1.02 ± 0.04; Fig. 2p,q). Importantly, compared with wild-type (WT) embryos and *miR-206* morphants, we found that VegfAa was not excessively expressed in embryos injected with *miR-206*-MO plus *sars*-mRNA (ari ± s.d. = 0.99 ± 0.09). These results indicated that the increase of VegfAa resulting from the suppression of *miR-206* can be rescued by the addition of *sars*-mRNA.

To examine differential regulation of *vegfaa* by *miR-1* and *miR-206*, we used the *luc* reporter construct containing WT and mutated *vegfaa*-3′UTR[12]. Results showed that the *luc* activity of the mutated *vegfaa* reporter whose seed sequence CATTCC had been mutated to CTAACC (*Zvegf-3′UTR*-mt1) was greatly increased (Fig. 3). Coinjection of the WT *vegfaa*-3′UTR reporter plus *miR-206*-MO restored the reduced luciferase expression to a level similar to that of embryos injected with mutant reporter (Fig. 3). However, coinjection of the WT *vegfaa*-3′UTR reporter plus *miR-1*-MO1 did not change the *luc* activity (Fig. 3), suggesting that only *miR-206*, but not *miR-1*, specifically targets *vegfaa*-3′UTR to mediate *vegfaa* expression.

Together, the above results indicated that *miR-1* and *miR-206* have distinctly different roles in the development of the ISV. Specifically, *miR-1* positively affects angiogenesis through *sars* regulation, whereas *miR-206* negatively affects angiogenesis independent of *sars* regulation.

***miR-1* represses SARS through direct targeting of *sars*-mRNA.** To further confirm that *sars*-3′UTR is a direct target of *miR-1*, we employed a target protector morpholino (TP-MO)[12,21,22], which is complementary to the *miR-1* target site (Fig. 4a), resulting in the inhibition of *miR-1* targeting on *sars*-3′UTR. We also constructed two plasmids in which the downstream of EGFP reporter was fused with either the full length of WT *sars*-3′UTR or the mutated sequence of *sars*-3′UTR. When we injected *egfp*-mRNA containing either WT *sars*-3′UTR or mutated *sars*-3′UTR into the one-cell stage, the GFP signal was observed in embryos at 24 hpf. The GFP signal was observed throughout the embryo in

the positive control group whose embryos were injected with *egfp*-mRNA plus control-MO (Fig. 4b), However, a significant reduction in GFP signal was observed in the trunk muscles of negative control group whose embryos were injected with *egfp*-mRNA containing WT *sars*-3′UTR by the presence of endogenous *miR-1* (Fig. 4c). Interestingly, we found that the GFP signal was not reduced in the trunk muscles of embryos injected with *egfp*-mRNA containing either the mutated *sars*-3′UTR plus control-MO (Fig. 4d) or WT *sars*-3′UTR plus *sars*-TP-MO (Fig. 4e), suggesting that *miR-1* silencing is abolished when the *miR-1*-target sequence on *sars*-3′UTR is blocked by *sars*-TP-MO. Furthermore, we found that injection of WT *sars*-3′UTR plus *miR-1*-MO1 could restore the reduced GFP signal caused by *miR-1* knockdown (Fig. 4f). However, injection of WT *sars*-3′UTR plus *miR-206*-MO could not restore the reduced GFP signal (Fig. 4g). In addition, western blot analysis demonstrated that the SARS protein level was increased (ari ± s.d. = 1.41 ± 0.06 versus ari ± s.d. = 1.01 ± 0.04 for control-MO-injected embryos), whereas the VegfAa protein level was decreased (ari ± s.d. = 0.39 ± 0.09 versus ari ± s.d. = 1.04 ± 0.02 for control-MO-injected embryos) in *sars*-TP-MO-injected embryos (Fig. 4h,i). Therefore, when the *miR-1* target site is blocked by *sars*-TP-MO, *sars*-mRNA can stabilize, resulting in the translation of more SARS, which in turn, reduces VegfAa.

To examine the specific effect of *sars*-TP-MO *in vivo* on *sars*-mRNA, we injected *sars*-TP-MO into embryos derived from transgenic line *Tg(fli-nGFP)*^{y7} and monitored the development of ISVs labelled by GFP. Compared with control group, the angiogenesis of embryos-injected *sars*-TP-MO was repressed (Fig. 4j versus k). This phenotype recapitulated the vascular defect

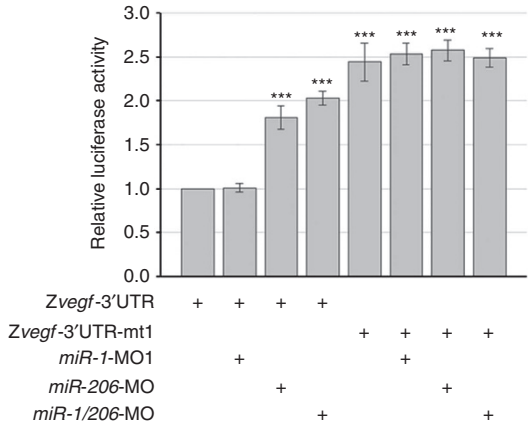

Figure 3 | The zebrafish *vegfaa* mRNA is regulated differently by *miR-1* and *miR-206*. Histograms presented the *luc* activity obtained from zebrafish embryos at 24 hpf. Plasmid pCS2^{+}-Z*vegf*-3′UTR served as a control group, and its *luc* activity was set to 1. The *luc* activity assay are calculated from three independent experiments and presented as mean ± s.d. ($n = 3$). Student's *t*-test was used to determine significant differences between each construct and control within each group (***$P < 0.005$).

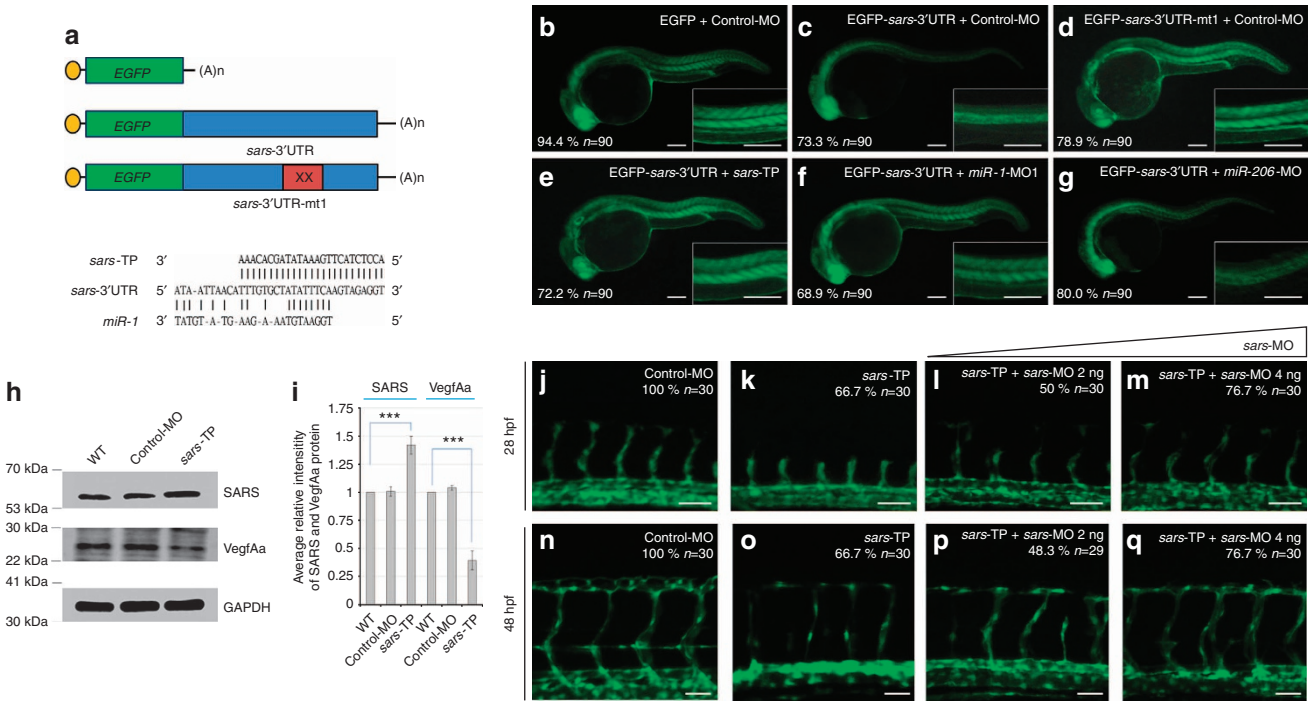

Figure 4 | Using morpholino target protector (TP) to show that *miR-1* represses zebrafish *sars*-3′UTR. (**a**) Sequence of the target site, cognate *sars*-TP-MO (*sars*-TP), and *miR-1* were indicated. The full length of *sars*-3′UTR was inserted downstream of an EGFP expression vector. (**b**) In the control group, the GFP signal was observed throughout the embryos injected with *egfp*-mRNA plus control-MO. (**c**) The GFP signal in truck somites, shown at right lower corner, was greatly reduced in embryos injected with control-MO plus *egfp*-mRNA containing WT *sars*-3′UTR. (**d**) The GFP signal in truck somite was restored when the *miR-1* target site on *sars*-3′UTR was mutated. (**e**) The GFP signal in truck somite was also restored in embryos injected with EGFP-WT *sars*-3′UTR plus *sars*-TP-MO. (**f**) The reduced GFP caused by EGFP-*sars*-3′UTR could be restored by coinjection of *miR-1*-MO1. (**g**) The reduced GFP caused by EGFP-*sars*-3′UTR could not be restored by coinjection of *miR-206*-MO. (**h**) Western blot analysis to detect the proteins of SARS and VegfAa in the WT, control-MO-injected and *sars*-TP-MO-injected embryos at 48 hpf. (**i**) The statistical analyses of the average relative intensities of SARS and VegfAa performed on densitometry from WT, control-MO-injected and *sars*-TP-MO-injected embryos after three independent experiments. Data are presented as mean ± s.d. ($n = 3$). Student's *t*-test was used to determine significant differences between each construct and control within each group (***$P < 0.005$). GAPDH served as an internal control. (**j**–**q**) Embryos derived from line *Tg(fli1:EGFP)* were injected with materials as indicated, and ISV patterns were observed at 28 and 48 hpf. Scale bar: (**b**–**g**) 300 μM; (**j**–**q**) 100 μM.

observed in the *miR-1* knockdown embryos (Fig. 4k versus 2b). However, this phenotype could be rescued by coinjecting an excessive amount of *sars*-MO (Fig. 4k versus l, m; Fig. 4o versus p, q). Unlike the *miR-1* morphants which were unable to continue development of blood vessels, the trunk vasculatures were almost completely formed in *sars*-TP/*sars*-MO-injected embryos. Ectopic sprouting of the tip cells was detected, which was similar to the phenotypes of *sars* morphants.

The *miR-1*/SARS pathway modulates *vegfaa* expression. This *miR-1*/SARS regulatory pathway is different from the *miR-1/206*/Vegf regulatory pathway proposed by Stahlhut *et al.*[12] in that they observed the promotion of *vegfaa* expression in *miR-1/206* double knockdown zebrafish embryos. However, although we have demonstrated that *miR-1* promotes angiogenesis through silencing SARS, it is unclear whether such effect is direct or whether the *miR-1*/SARS regulatory pathway acts as an upstream modulator of *vegfaa* expression to, in turn, promote angiogenesis in somitic cells. To address this question, we quantified *vegfaa*-mRNA in 48 hpf embryos injected separately with *miR-1*-MO1 and *sars*-mRNA. Results showed that the expression of *vegfaa*-mRNA was greatly reduced in the *miR-1* morphants and *sars*-overexpressed embryos (Fig. 5a). Second, western blot analysis showed that VegfAa was also reduced in *miR-1* morphants, whereas VegfAa was increased both in *miR-206*-MO- and *miR-1/206*-MO-injected embryos (Fig. 5b). Similar results were obtained in the mammalian system because we found that overexpression of *miR-1* in cell line C2C12 caused a 46% decrease of SARS, and a 29% increase of VegfAa protein, whereas overexpression of mouse *sars*-mRNA caused a 41% increase of SARS and a 45% decrease of VegfAa (Fig. 5c,d). Thus, we concluded that VegfAa was reduced when *miR-1* was absent, but that it was increased when SARS was absent, suggesting that *miR-1* reduces SARS, which, in turn, results in the increase of VegfAa. In addition, as determined by enzyme-linked immunosorbent assay (ELISA), we found that the overexpression of pre-*miR-1* in C2C12 cells caused a 45% increase of VegfAa expression (Fig. 5e), whereas, on the other hand, overexpression of SARS caused a 40% decrease of VegfAa expression (Fig. 5e), suggesting that the secretion of VegfAa from C2C12 cells can be affected by either *miR-1* or SARS. We also observed that the nuclear content of SARS protein was increased by 28% and 75% in the knockdown of *miR-1* and overexpression of SARS, respectively, during zebrafish embryogenesis (Fig. 5f). These data supported Xu *et al.*[20] who proved that SARS negatively regulates *vegfaa* transcription through entering the nucleus. Together, we proposed that *miR-1* functions to reduce the protein level of SARS in somites in order to keep excessive SARS from entering the nucleus, which, in turn, promotes *vegfaa* expression in blood vessels. This fact is consistent between zebrafish *in vivo* study and mammalian *in vitro* study.

Interestingly, we performed qPCR to quantify the expression levels of *miR-1* and *miR-206* in embryos from 12 to 32 hpf to determine any differences in the timing of expression levels of *miR-1* and *miR-206*. Results showed that the expression level of *miR-1* was gradually increased during 12–20 hpf. But, the value was dramatically increased from 20 to 32 hpf (Supplementary Fig. S7A,B). However, the expression level of *miR-206* was insignificantly changed during these stages (Supplementary Fig. S7A,B). In addition, we determined *miR-1* and *miR-206* copy numbers at different developmental stages which are based on the relative value against the known copies in a genome sequence, such as U6 (refs 23–25). The relative copy number of *miR-1* per 100 U6 was gradually increased during 12–20 hpf (Supplementary Fig. S7C). Particularly, the value was dramatically increased from 20 to 32 hpf (Supplementary Fig. S7C). In contrast, the relative copy number of *miR-206* per 100 U6 was insignificantly changed during these stages (Supplementary Fig. S7C). Taken together, this evidence indicates that the amount of *miR-1* is greatly increased from 20 to 32 hpf, whereas that of *miR-206* remains insignificant throughout these stages of development. Moreover, the great increase of VegfAa during 24–30 hpf, which was reported by Liang *et al.*[26], might be responsible for the continuous increase of *miR-1*/SARS/VegfAa axis, but not *miR-206*/VegfAa axis. Therefore, we can safely conclude that differences in the timing of repression of *miR-1* and *miR-206* occur during embryogenesis, suggesting, in turn, that the *miR-1*/SARS/VegfAa pathway increasingly affects embryonic angiogenesis at late developmental stages in somitic cells.

Discussion

The non-canonical activity of SARS in somites is involved in vascular development by modulating the expression of *vegfaa*[14]. Xu *et al.*[20] identified a nuclear localization signal sequence embedded in the UNE-S domain at the carboxyl-terminus of SARS, which can help SARS enter the nucleus and repress *vegfaa* expression. In the present report, we found that *miR-1*, but not *miR-206*, can specifically repress SARS expression by targeting the 3′UTR of *sars*-mRNA. Our data also proved that either excessive expression of SARS or knockdown of *miR-1* in zebrafish embryos can increase the amount of SARS entering the nucleus. The rescue experiment showed that knockdown of SARS in the *miR-1*-MO1-injected embryos could rescue Se vessel defects induced by *miR-1*-MO1. Therefore, it was proposed that *miR-1* positively regulates VegfAa expression by limiting the amount of SARS protein in somites.

Our data shows that, first, the *vegfaa*-3′UTR is regulated differently by *miR-1* and *miR-206*; second, overexpression of SARS can rescue the elevated numbers of endothelial cells caused by *miR-206* knockdown; third, SARS is increased, but VegfAa is reduced, in *miR-1*-MO-injected embryos, whereas SARS remains unchanged, but VegfAa is increased, in *miR-206*-MO-injected embryos; and finally, SARS is a negative regulator of VegfAa. Therefore, we proposed that *miR-1* has a regulatory role opposite to that of *miR-206* through directly controlling the level of SARS protein, but indirectly controlling the level of VegfAa protein level, during zebrafish angiogenesis. That is, although the *miR-1*/SARS regulatory pathway promotes embryonic angiogenesis by the upstream modulation of *vegfaa*, *miR-206* has an anti-angiogenic role by directly controlling VegfAa protein level.

We noticed that the similarity of angiogenic defects between those caused by *miR-206* single knockdown embryos and *miR-1/206* double knockdown embryos agrees with Stahlhut *et al.*[12] who reported that the number of endothelial cells in *miR-1/206*-MO-injected embryos was increased. However, the angiogenic phenotypes caused by *miR-1* single knockdown were totally masked by those of *miR-1/206* double knockdown. Although the reason for this needs further clarification, we suggested that *miR-206* can directly regulate VegfAa protein level in somitic cells. In contrast, we further suggested that the *miR-1*/SARS pathway may have the effect of fine-tuning angiogenesis, particularly as *miR-1* must regulate the level of SARS protein before it can regulate the level of VegfAa (Fig. 6).

miR-1 and *miR-206* are evolutionarily conserved *miRNA*s of highly similar sequence. Their seed sequences are identical and their sequences outside the seed exist only four nt differences. As shown in Supplementary Fig. S4, based on the theoretical prediction by bioinformatics analysis, the degree of complementarity between *miR-1* and *sars*-3′UTR, as well as *miR-206* and *sars*-3′UTR, is insignificant. However, based on *in vivo*

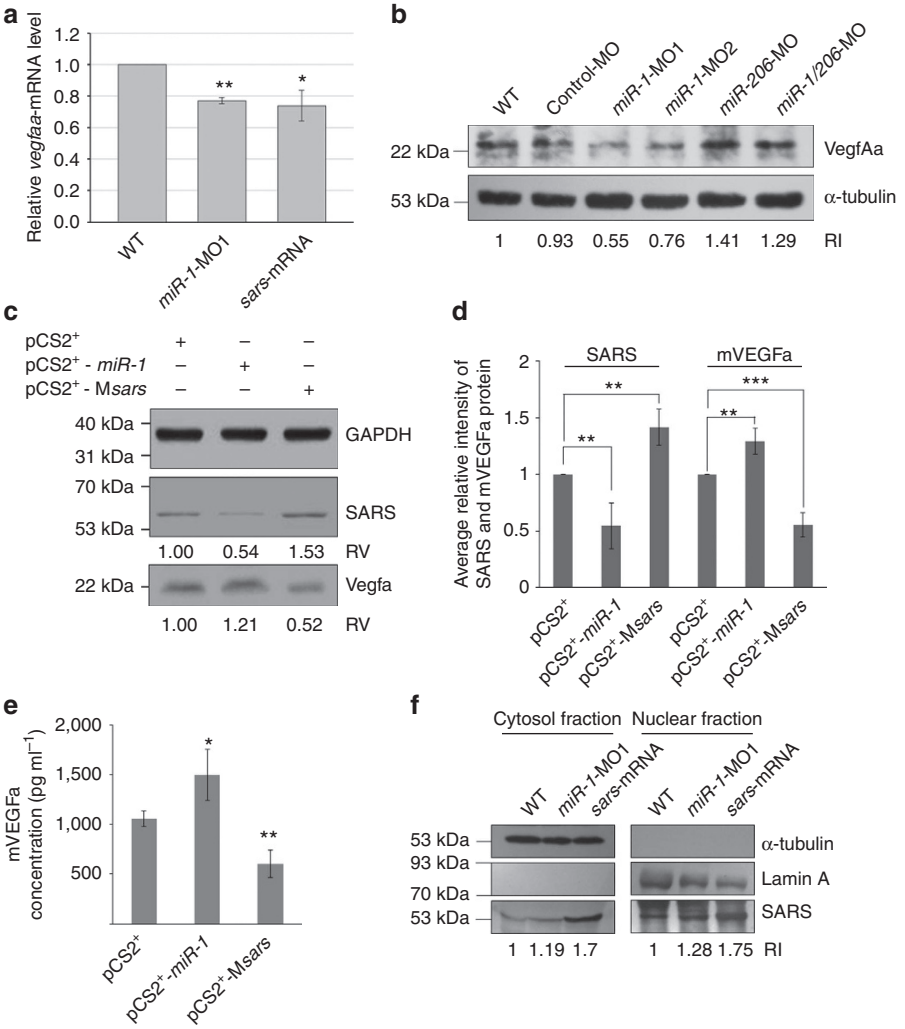

Figure 5 | Knockdown of *miR-1* and overexpression of *sars* result in downregulating the expression of *vegfaa*. (**a**) The statistical analysis of quantitative RT-PCR of *vegfaa*-mRNA level in the embryos injected with *miR-1*-MO1 (8 ng) and *sars*-mRNA (300 pg) at 48 hpf. The intensity of *vegfaa*-mRNAs in WT served as control and was set as 1. Data are presented as mean ± s.d. ($n = 3$). Student's *t*-test was used to determine significant differences between each group (*$P < 0.05$, **$P < 0.01$). (**b**) Western blot analysis of VegfAa protein level in zebrafish embryos was presented. The relative intensities (RI) of VegfAa protein among WT, Control-MO-, *miR-1*-MO1-, *miR-1*-MO2-, *miR-206*-MO- and *miR-1/miR-206*-MO-injected embryos were as indicated. The protein level of α-tubulin served as an internal control for loading amount of proteins. (**c**) Western blot analyses of total proteins extracted from cell line C2C12 which was individually transfected with pCS2$^+$ vector, pCS2$^+$-*miR-1* and pCS2$^+$-M*sars* (mouse *sars* cDNA). The relative intensity (RI) of SARS and VegfAa proteins among pCS2$^+$-, pCS2$^+$-*miR-1*- and pCS2$^+$-M*sars*-transfected cells were indicated. The protein level of GAPDH served as an internal control. (**d**) Statistical analyses of the average relative intensity (ari) of SARS and VegfAa proteins from each group were presented. Data are calculated from three independent experiments and presented as mean ± s.d. ($n = 3$). Student's *t*-test was used to determine significant differences between each group (**$P < 0.01$, ***$P < 0.005$). (**e**) ELISA to determine the amount of VegfAa secreted from C2C12 when pre-*miR-1* and SARS protein were overexpressed. Data are calculated from three independent experiments and presented as mean ± s.d. ($n = 3$). Student's *t*-test was used to determine significant differences between each group (*$P < 0.05$, **$P < 0.01$). The RI of mVegfa protein among in each group was as indicated. (**f**) Western blot analysis of SARS protein level in the cytosol fraction and nuclear fraction extracted from WT, *miR-1*-MO1- and *sars*-mRNA-injected embryos were as indicated. The protein levels of α-tubulin and Lamin A were used as internal control of cytosol fraction and nuclear fraction, respectively.

experiments using *luc* assay in zebrafish embryos, as shown in Fig. 1e, we clearly demonstrated that simultaneous knockdown of *miR-1* and *miR-206* restores mt2 expression, but not individual knockdown of *miR-1* or *miR-206*. Meanwhile, mutated construct mt2 is targeted equally, or redundantly, by these two *miRNAs*, whereas mt3 is targeted specifically by *miR-206*. Thus, we conclude that the endogenous *sars*-3′UTR target sequence (outside of seed) is refractory to *miR-206* targeting, despite additional *miR-206* complementarity. Instead, *sars*-3′UTR target sequence is specifically targeted by *miR-1*. This result actually proved that the sequences in the neighbourhood of the seed are involved in the specificity of *miRNA* differential targeting, suggesting that the sequences outside the seed are critical for targeting selection. In addition that many principles for *miRNA* targeting, such as the local context of the target site can influence the efficiency of *miRNA* regulation[4,27], the present study demonstrated that the two *miRNAs* with the same seed and strong similarities outside the seed do regulate different targets which provides important insight into new regulatory rules outside the seed *in vivo*.

Many reports revealed that *miR-1* is considered to be a tumour suppressor as overexpression of *miR-1* can repress tumour growth[28–30]. However, other studies showed that *miR-1* can induce cell proliferation and thus serve as an onco-*miRNA* in

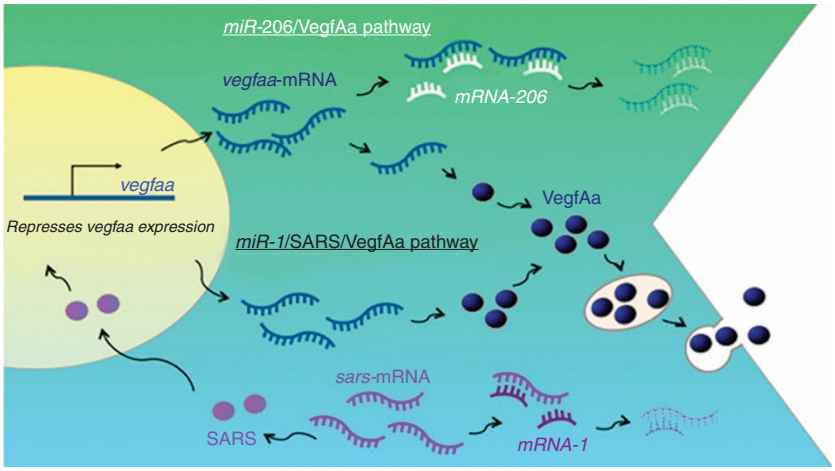

Figure 6 | Schematic representation showing the opposing roles played by *miR-1* and *miR-206* in the regulation of SARS and VegfAa. In somitic cells, *miR-1* serves as a pro-angiogenic modulator by inducing VegfAa expression through repressing SARS expression, whereas *miR-206* serves as an anti-angiogenic modulator by directly repressing *vegfaa* expression. These two pathways control the secreted levels of VegfAa from the somites to regulate angiogenesis.

multiple myeloma plasma cell neoplasms[31,32]. Thus, the role of *miR-1* in tumour growth might be cancer cell type-dependent because different cell lines express different Vegf-related *miRNAs*[33]. On the other hand, overexpression of *miR-1/206* during muscle regeneration in rat can induce angiogenesis[17]. This result is consistent with the pro-angiogenic character of *miR-1*, whereas, at the same time, it conflicts with the role of *miR-206*. Angiogenesis is a crucial and delicate bioprocess from the standpoints of physiology and pathology, including development, regeneration, inflammation and tumour formation. As Vegf expression is a pivotal factor, it should be well regulated[34,35]. We hypothesized that VegfAa is variously regulated by *miR-1/206* according to the cell type and physiological condition.

We have shown that *miR-1* and *miR-206* have opposing roles in the regulation of *vegfaa* in somites during zebrafish embryogenesis (Fig. 6). This contrasting functionality sheds more light on the complicated mechanisms underlying *miRNA*-modulated angiogenesis during embryonic development. Future studies will focus on the regulatory roles of *miR-1* and *miR-206* in angiogenesis under different physiological conditions, as well as the specific interactions between *miR-1/206* and their target genes in terms of targeting mechanism and physiological relevance.

Methods

Zebrafish husbandry and microscopy observation. WT zebrafish (*Danio rerio*), transgenic lines *Tg(fli1:EGFP)*^{y1} (ref. 36) and *Tg(fli1:nuclearEGFP)*[37] provided by the Lawson's Lab (UMASSMED) were maintained in aquaria according to standard procedures described by Westerfield[38]. The experiments and treatments of this animal have been reviewed and approved by the National Taiwan University Institutional Animal Care and Use Committee with ethics approval number: NTU-101-EL-115. Fluorescence was visualized with a fluorescent stereomicroscope (MZ FLIII, Leica) and a confocal spectral microscope (TCS SP5, Leica).

MOs used to perform knockdown experiments. The mRNAs were synthesized by the SP6 Message Machine Kit (Ambion). All MOs were purchased from Gene Tools (USA) and prepared according to the protocol published by Gene Tools. The sequence of the MOs we used were as follows: *miR-1*-MO1 (AATACATACTT CTTTACATTCCA)[12], *miR-1*-MO2 (CATATGGGCATATAAAGAAGTATGT), *miR206*-MO (GATCTCACTGAAGCCACACACTTCC), *miR-1/206*-MO: (AGC CACACACTTCCTTACATTCCAT), *sars*-TP-MO (ACCTCTACTTGAAATA TAGCACAAA), Control- MO (CCTCTTACCTCAGTTACAATTTATA), *miR-1*-5mis-MO (AATAAATAATTGTTTAAATTACA), and *miR-206*-5mis-MO (GATATCAATGAACCCAAACAATTCC) (the mismatched nt are underlined).

Whole-mount *in situ* hybridization. After we cloned the partial DNA fragments of the desired gene, the probes were Digoxigenin (DIG)-labelled. After permeabilization, embryos were hybridized overnight. Then, embryos were incubated with anti-DIG antibody (Roche; 1:8,000), stained and observed under a fluorescent stereomicroscope (MZ FLIII, Leica)[39]. To detect expression of mature *miR-1* and *miR-206*, DIG-labelled LNA probes were purchased from Integrated DNA technologies. The procedure of WISH was performed according to the protocol published by Exiqon.

Western blot analysis. Embryos were dechorionized, deyolked and lysed in whole-cell extract buffer (Hepes 20 mM; NaCl 0.2 M; TritonX100 0.5%; glycerol 20%; EDTA 1mM; and EGTA 1mM) containing the proteinase inhibitor cocktail (Roche). The lysates proteins were separated on SDS–PAGE and blotted with corresponding antibodies. The number of embryos used for each lane of gel ranged from 30 to 60 depending on the amount of examined proteins[39,40]. Antibodies against SARS (Abnova; H00006301-MO1; 25 μg ml^{-1}; 1:1,000), GADPH (Santa Cruz; SC-32233; 100 μg ml^{-1}; 1:1,000), α-tubulin (Sigma-Aldrich; T6199; 1 mg ml^{-1}; 1:1,000), Vegfa (Abnova; MAB0294; 0.1 μg μl^{-1}; 1:1,000), VegfAa (R & D; AF1247; 0.1 μg ml^{-1}; 1:1,000), Anti-mouse-HRP (Santa Cruz; SC-2031; 200 μg per 0.5 ml; 1:5,000), and Anti-rabbit-HRP (Santa Cruz; SC-2004; 200 μg per 0.5 ml; 1:5,000) were used. Full scans of Western blots are shown in Supplementary Figs S8–S11.

Plasmid constructs. The open reading frame (ORF) of *sars* from zebrafish (*Zsars*) and mice (*Msars*) were cloned from zebrafish embryos and mouse C2C12 cell line by PCR, respectively. The ORF of *Zsars* and *Msars* was, respectively, inserted into pCS2$^+$ to generate pCS2$^+$-*Zsars* and pCS2$^+$-*Msars*, respectively. The pre-*miR-1* and pre-*miR-206* were cloned from zebrafish genomic DNA by PCR. The pre-*miR-1* and pre-*miR-206* were inserted into pCS2$^+$ to generate pCS2$^+$-*miR-1* and pCS2$^+$-*miR-206*. The 3′UTR of *Zsars*, *Msars* and Human *sars* (*Hsars*) were cloned from zebrafish embryos, mouse C2C12 cell line and Human HEK293T cell line. The 3′UTR of *Zsars*, *Msars* and *Hsars* was, respectively, inserted into phRG-TK to generate phRG-TK-*Zsars*-3′UTR, phRG-TK-*Msars*-3′UTR and phRG-TK-*Hsars*-3′UTR. The 3′UTR of *Zsars* was inserted into phRL-*myf5* to generate phRL-*myf5*-*Zsars*-3′UTR.

In the *in vivo* luciferase experiment, we used PCR to mutate the *miR-1* target sequences of *Zsars*-3′UTR, three mutated constructs were generated, as follows: *Zsars*-3′UTR-mt1 (ATAATTAACATTTGTGCTATATTTCA is mutated to ATAATTAACATTTGTGCTATATAGGT); *Zsars*-3′UTR-mt2 (ATAATTAACAT TTGTGCTATATTTCA mutated to TATTAATTGTAAACACGTATATTTCA), and *Zsars*-3′UTR-mt3 (ATAATTAACATTTGTGCTATATTTCA mutated to CCAATCAACATTTGCGCTATATTTCA). These mutated fragments were then inserted into phRL-*myf5* to generate phRL-*myf5*-*Zsars*-3′UTR-mt1, phRL-*myf5*-*Zsars*-3′UTR-mt2 and phRL-*myf5*-*Zsars*-3′UTR-mt3 individually. In the *in vivo* reporter experiment, the DNA fragments of *Zsars*-3′UTR and *Zsars*-3′UTR-mt1 were inserted into pCS2$^+$-EGFP to generate pCS2$^+$-EGFP-*Zsars*-3′UTR and pCS2$^+$-EGFP- *Zsars*-3′UTR-mt1, respectively.

Non-canonical mutant SARS T429A. SARS T429A is a SARS mutant whose canonical activity is blocked by the replacement of threonine located at 429 by Alanine (T429A), resulting in the inhibition of enzymatic activity that catalyses aminoacylation of transfer RNA for serine[14]. Although SARS T429A lacked canonical activity, it could still suppress the abnormal branching of ISVs in *sars*

mutant fish (ko095)[14]. Following this logic, we used SARS T429A in this study to confirm whether the non-canonical activity of SARS is involved in *miR-1/206*-mediated vascular development. Plasmids containing WT *sars* or *sars* mutant T429A were gifts from Prof. Kawahara (RIKEN[14]). After the coding regions were amplified by PCR, the products were then inserted into pCS2$^+$ expression vector to generate mRNAs *in vitro* using the mMESSAGE mMACHINE SP6 Kit (Ambion).

Dual luciferase assay. Dual *luc* reporter assay was carried out in cell lines HEK-293T and C2C12 following the standard protocol recommended by Promega with some modifications. In the control group, we co-transfected 20 ng of plasmid pGL3-TK, which served as an internal control, and 100 ng of each examined plasmid. In the experimental group, we cotransfected 20 ng of pGL3-TK, 100 ng of each examined plasmid plus 1.25 μg of plasmid pCS2$^+$-*miR-1* or pCS2$^+$-*miR-206*. For dual *luc* reporter assay in zebrafish embryos, we coinjected 5 ng μl^{-1} of pGL3-TK, which also served as an internal control, and 5 ng μl^{-1} of phRL-*myf5*, as described above, to serve as a control group, whereas we coinjected 5 ng μl^{-1} of pGL3-TK and 5 ng μl^{-1} of other *luc* reporter constructs to serve as an experimental group[41]. For each experiment, we randomly collected 30 embryos from 50 to 100 injected embryos and divided them into three groups ($n = 10$ per group) to carry out *in vivo* luciferase assays. Data for each experiment were the average of three groups. The final data, presented as mean ± s.d., were an average of three independent experiments, which were carried out on different days.

Enzyme-linked immunosorbent assay. The supernatants collected from C2C12 cells transfected separately with *miR-1* and M*sars* for 48 h were assayed using an ELISA kit for mVegf (eBioscience) according to the manufacturer's instructions.

qPCR. For each experiment, we collected 100 embryos in 500 ml of Trizol Reagent (Invitrogen). Total RNAs were isolated according to the manufacturer's instructions. For qPCR, first-strand cDNA was generated using 1 mg of total RNA. Both cDNA concentrations were adjusted to 200 ng ml^{-1}, and qPCR was performed using the 7900HT Fast Real-Time PCR System (Applied Biosystems) according to the manufacturer's instructions. Forward and reverse primers describe by Fukui *et al.*[14] were used, as follows: forward primer TCCTGTGTGGTTCTCATGC and reverse primer TGCATTCACACTTGGTGTGTTC for amplifying zebrafish *vegfaa*; forward primer CTCCTCTTGGTCGCTTTGCT and reverse primer CCGATT TTCTTCTCAACGCTCT for amplifying *ef1a*. Expression levels were determined by comparison with a standard curve from total RNAs isolated from WT embryos.

For quantitative detection of *miR-1* and *miR-206* in embryos at 12, 16, 20, 24, 28 and 32 hpf, the cDNAs of *miR-1* and *miR-206* were synthesized by *miR-1*-RT primer (CTCAACTGGTGTCGTGGAGTCGGCAATTCAGTTGAGATACAT) and *miR-206*-RT primer (CCATCATGCTCTCGACCTGTCCGATCACGACGA GAGCATGATGGCCACAC). For qPCR of *miR-1*, the primers were *miR-1*-F (GCTATGGAATGTAAAGAAGTATGTAT) and *miR-1*-R (CTCAACTG-GTGTCGTGGAGTC). For qPCR of *miR-206*, the primers were *miR-206*-F (GTTATGGAATGTAAGGAAGTGTGTGG) and *miR-206*-R (CCATCATGCTC TCGACCTGTC). The internal controls for *miR-1* and *miR-206* were *β-actin* (β-actin-1072F:GGATCGGTGGCTCCATCTT; *β-actin*-1144R:TCATCGTA CTC- CTGCTTGCTGAT) and *EF1α* (*EF1α*-1330F: CTCCTCTTGGTCGCTTT GCT; *EF1α*-1411R: CCGATTTTCTTCTCAACGCTCT). To compare the relative expression levels of *miR-1* and *miR-206* at each stage, the expression levels of *miR-1* and *miR-206* at 12 hpf were set as 1.

To determine the copy number of *miR-1* and *miR-206*, zebrafish U6 snRNA was used as endogenous control. Specific plasmids were constructed for *miR-1*, *miR-206* and U6 by cloning products for real-time PCR. Knowing the size of the plasmid that contains the gene of interest, the number of grams/molecule and copy number can be calculated as follows:

Weight in Daltons (g mol^{-1}) = (bp of double-stranded product) × (330 Da × 2nt per bp). Hence, (g mol^{-1})/Avogadro's number = g per molecule = copy number.

Knowing the copy number and concentration of plasmid DNA, the precise number of molecules added to subsequent real-time PCR can be calculated, thus providing a standard for specific cDNA quantification. Real-time PCR was carried out in a MicroAmp Optical 96-well plate using power SYBR Green PCR Master Mix (Applied Biosystems), with 2 μl cDNA or Specific control DNA (10^2–10^6 copies) in each well. PCR reactions were monitored in real time using the ABI 7900HT Fast Real-time PCR system (Applied Biosystems). The thermal cycling conditions for real-time PCR were 50 °C for 2 min, then 95 °C for 10 min and 40 cycles of denature (95 °C, 15 s) and annealing/extension (60 °C, 60 s). A standard curve was drawn by plotting the natural log of the threshold cycle (CT) against the natural log of the number of molecules. CT was calculated under default settings for real-time sequence detection software (Applied Biosystems). The equation drawn from the graph was used to calculate the precise number of specific cDNA molecules tested in the same reaction plate as the standard. For qPCR of U6, the primers were U6-F (ACTAAAATTGGAACGATACAGAGA) and U6-R (AAAGA TGGAACGCTTCACG). To compare the relative expression levels of *miR-1* and *miR-206* at each stage, the expression levels of *miR-1* and *miR-206* which normalized to U6 at 12 hpf were set as 1.

Statistical analysis. Data were averaged from three independent experiments and presented as mean ± s.d., and difference levels were analysed using Student's *t*-test. $^*P < 0.05$, $^{**}P < 0.01$ and $^{***}P < 0.005$ indicated the significant difference levels.

References

1. Djuranovic, S., Nahvi, A. & Green, R. A parsimonious model for gene regulation by *miRNAs*. *Science* **31,** 550–553 (2011).
2. Huntzinger, E. & Izaurralde, E. Gene silencing by microRNAs: contributions of translational repression and mRNA decay. *Nat. Rev. Genet.* **12,** 99–110 (2011).
3. Fabian, M. R., Sonenberg, N. & Filipowicz, W. Regulation of mRNA translation and stability by microRNAs. *Annu. Rev. Biochem.* **79,** 351–379 (2010).
4. Bartel, D. P. MicroRNAs: target recognition and regulatory functions. *Cell* **136,** 215–233 (2009).
5. Rajewsky, N. MicroRNA target predictions in animals. *Nat. Genet.* **38,** S8–S13 (2006).
6. Sweetman, D. *et al.* Specific requirements of MRFs for the expression of muscle specific microRNAs, miR-1, miR-206 and miR-133. *Dev. Biol.* **321,** 491–499 (2008).
7. Chen, J. F. *et al.* The role of microRNA-1 and microRNA-133 in skeletal muscle proliferation and differentiation. *Nat. Genet.* **38,** 228–233 (2006).
8. Nohata, N., Hanazawa, T., Enokida, H. & Seki, N. MicroRNA-1/133a and microRNA-206/133b clusters: dysregulation and functional roles in human cancers. *Oncotarget* **3,** 9–21 (2012).
9. Rao, P. K., Kumar, R. M., Farkhondeh, M., Baskerville, S. & Lodish, H. F. Myogenic factors that regulate expression of muscle-specific microRNAs. *Proc. Natl Acad. Sci. USA* **103,** 8721–8726 (2006).
10. Cacchiarelli, D. *et al.* MicroRNAs involved in molecular circuitries relevant for the Duchenne muscular dystrophy pathogenesis are controlled by the dystrophin/nNOS pathway. *Cell Metab.* **12,** 341–351 (2010).
11. Anderson, C., Catoe, H. & Werner, R. MIR-206 regulates connexin43 expression during skeletal muscle development. *Nucleic Acids Res.* **34,** 863–5871 (2006).
12. Stahlhut, C., Suárez, Y., Lu, J., Mishima, Y. & Giraldez, A. J. MiR-1 and miR-206 regulate angiogenesis by modulating VegfAa expression in zebrafish. *Development* **139,** 4356–4364 (2012).
13. Mishima, Y. *et al.* Zebrafish miR-1 and miR-133 shape muscle gene expression and regulate sarcomeric actin organization. *Genes Dev.* **23,** 619–632 (2009).
14. Fukui, H., Hanaoka, R. & Kawahara, A. Noncanonical activity of seryl-tRNA synthetase is involved in vascular development. *Circ. Res.* **104,** 1253–1259 (2009).
15. Javerzat, S., Auguste, P. & Bikfalvi, A. The role of fibroblast growth factors in vascular development. *Trends Mol. Med.* **8,** 483–489 (2002).
16. Poole, T. J., Finkelstein, E. B. & Cox, C. M. The role of FGF and VEGF in angioblast induction and migration during vascular development. *Dev. Dyn.* **220,** 1–17 (2001).
17. Nakasa, T. *et al.* Acceleration of muscle regeneration by local injection of muscle-specific microRNAs in rat skeletal muscle injury model. *J. Cell Mol. Med.* **14,** 2495–2505 (2010).
18. Hsu, R. J., Yang, H. J. & Tsai, H. J. Labeled microRNA pull-down assay system: an experimental approach for high-throughput identification of microRNA-target mRNAs. *Nucleic Acids Res.* **37,** e77 (2009).
19. Rehmsmeier, M., Steffen, P., Hochsmann, M. & Giegerich, R. Fast and effective prediction of microRNA/target duplexes. *RNA* **10,** 1507–1517 (2004).
20. Xu, X. *et al.* Unique domain appended to vertebrate tRNA synthetase is essential for vascular development. *Nat. Commun.* **3,** 681 (2012).
21. Choi, W. Y., Giraldez, A. J. & Schier, A. F. Target protectors reveal dampening and balancing of Nodal agonist and antagonist by miR-430. *Science* **318,** 271–274 (2007).
22. Staton, A. A. & Giraldez, A. J. Use of target protector morpholinos to analyze the physiological roles of specific *miRNA*-mRNA pairs in vivo. *Nat. Protoc.* **6,** 2035–2049 (2011).
23. Choong, M. L., Yang, H. H. & McNiece, I. MicroRNA expression profiling during human cord blood-derived CD34 cell erythropoiesis. *Exp. Hematol.* **4,** 551–564 (2007).
24. Corney, D. C., Flesken-Nikitin, A., Godwin, A. K., Wang, W. & Nikitin, A. Y. MicroRNA-34b and microRNA-34c are targets of p53 and cooperate in control of cell proliferation and adhesion independent growth. *Cancer. Res.* **18,** 8433–8438 (2007).
25. Shell, S. *et al.* Let-7 expression defines two differentiation stages of cancer. *Proc. Natl Acad. Sci. USA* **104,** 11400–11405 (2007).
26. Liang, D. *et al.* The role of vascular endothelial growth factor (VEGF) in vasculogenesis, angiogenesis, and hematopoiesis in zebrafish development. *Mech. Dev.* **108,** 29–43 (2001).
27. Grimson, A. *et al.* MicroRNA targeting specificity in mammals: determinants beyond seed pairing. *Mol. Cell* **27,** 91–105 (2007).

28. Rao, P. K. *et al.* Distinct roles for miR-1 and miR-133a in the proliferation and differentiation of rhabdomyosarcoma cells. *FASEB J.* **24,** 3427–3437 (2010).
29. Kojima, S. *et al.* Tumour suppressors miR-1 and miR-133a target the oncogenic function of purine nucleoside phosphorylase (PNP) in prostate cancer. *Br. J. Cancer* **106,** 405–413 (2012).
30. Kawakami, K. *et al.* The functional significance of miR-1 and miR-133a in renal cell carcinoma. *Eur. J. Cancer* **48,** 827–836 (2012).
31. Gómez-Benito, M. *et al.* EVI1 controls proliferation in acute myeloid leukaemia through modulation of miR-1-2. *Br. J. Cancer* **103,** 1292–1296 (2010).
32. Gutiérrez, N. C. *et al.* Deregulation of microRNA expression in the different genetic subtypes of multiple myeloma and correlation with gene expression profiling. *Leukemia* **24,** 629–637 (2010).
33. Hua, Z. *et al. MiRNA*-directed regulation of VEGF and other angiogenic factors under hypoxia. *PLoS One* **1,** e116 (2006).
34. Ferrara, N., Gerber, H. P. & LeCouter, J. The biology of VEGF and its receptors. *Nat. Med.* **9,** 669–676 (2003).
35. Olsson, A. K., Dimberg, A., Kreuger, J. & Claesson-Welsh, L. VEGF receptor signaling – in control of vascular function. *Nat. Rev. Mol. Cell Biol.* **7,** 359–371 (2006).
36. Lawson, N. D. & Weinstein, B. M. In vivo imaging of embryonic vascular development using transgenic zebrafish. *Dev. Biol.* **248,** 307–318 (2002).
37. Roman, B. L. *et al.* Disruption of acvrl1 increases endothelial cell number in zebrafish cranial vessels. *Development* **129,** 3009–3019 (2002).
38. Westerfield, M. *The Zebrafish Book. A Guide for the Laboratory Use of Zebrafish (Danio rerio)* Eugene, OR (University of Oregon Press, 2000).
39. Lee, H. C., Tseng, W. A., Lo, F. Y., Liu, T. M. & Tsai, H. J. FoxD5 mediates anterior-posterior polarity through upstream modulator Fgf signaling during zebrafish somitogenesis. *Dev. Biol.* **336,** 232–245 (2009).
40. Link, V., Shevchenko, A. & Heisenberg, C. P. Proteomics of early zebrafish embryos. *BMC Dev. Biol.* **6,** 1 (2006).
41. Lin, C. Y. *et al.* MicroRNA-3906 regulates fast muscle differentiation through modulating the target gene homer-1b in zebrafish embryos. *PLoS One* **8,** e70187 (2013).

Acknowledgements

We are grateful to Ms Yi-Chun Chuang and Ms Ya-Chan Yang, staffs of TC5, College of Life Science, NTU, for helping with the confocal laser scanning microscopy. This work was supported by the National Science Council, Taiwan (102-2313-B-002-018-MY3).

Author contributions

C.-Y.L., H.-C.L., C.-Y.F. and H.-J.T. conceived the study and analysed *in vitro* and *in vivo* experiments; C.-Y.L. designed and constructed the plasmids; H.-C.L. and W.-J.H. performed *in vivo* experiments; C.-Y.F. and Y.-Y.D. carried out *in vitro* analysis; C.-Y.L. and J.-S.C. performed *luc* assay and WISH; H.-C.L. and C.-Y.F. carried out TP experiment; Y.-Y.D. and M.-H.L. performed western blot analysis; and C.-Y.L., H.-C.L. and H.-J.T. wrote the manuscript. Research idea was proposed by H.-J.T. and grant was under by H.-J.T.

Additional information

Supplementary Information accompanies this paper at http://www.nature.com/naturecommunications

Competing financial interests: The authors declare no competing financial interests.

Reprints and permission information is available online at http://npg.nature.com/reprintsandpermissions/

How to cite this article: Lin, C.-Y. *et al.* miR-1 and miR-206 target different genes to have opposing roles during angiogenesis in zebrafish embryos. *Nat. Commun.* 4:2829 doi: 10.1038/ncomms3829 (2013).